

# Optical properties of yttrium oxyhydrides: A comparative analysis with experiment

E. Strugovshchikov\* and A. Pishtshev†

*Institute of Physics, University of Tartu, Tartu, Estonia.*

S. Karazhanov

*Department for Solar Energy, Institute for Energy Technology, Kjeller, Norway*

(Dated: January 7, 2022)

Based on the results of computational simulations, the research addresses a broad range of electronic and optical properties which are typical for two most stable compositions of the yttrium oxyhydride,  $Y_4H_{10}O$  and YHO. Emphasis was placed on characteristics of thin films of different structural phases. Macroscopic optical properties were deduced and analyzed within the conventional scheme that utilizes the knowledge of refractive index, absorption, transmittance and reflectance spectra. Our major goal was two-fold: First, to provide modeling and description of optical spectra for various single- and bi-phase oxyhydride compositions, and second, to conduct comparative analysis that would be powerful enough to explain the features of the experimentally measured transmittance spectra. In the context of nonlinear optics, for the  $P-43m$  noncentrosymmetric cubic structure of  $Y_4H_{10}O$  we evaluated a frequency profile of the second-order susceptibility  $\chi^{(2)}(2\omega)$  and showed that the bulk  $Y_4H_{10}O$  may exhibit a rather considerable optical nonlinearity.

## I. INTRODUCTION

Generally, oxyhydrides relate to novel multi-anion materials that suggest a number of useful functionalities applicable in modern technology of optical and electronic smart microdevices [1, 2]. Chemical design of oxyhydrides was initiated more than 20 years ago [3–6]; it originates from the idea of improving several key properties of various metal hydrides. It was in the conducted research work revealing that the incorporation of oxygen into the hydride lattice not only reinstates stoichiometry through the regularization of hydrogen host positions, but also expands chemical potential of a modifiable metal-hydride system through the direct interactions with oxygen [3–8]. In the bulk structure, such procedure of partial oxidation becomes irreversible under normal conditions because new chemical configuration is secured by the formation of specifically-ordered lattice geometries [9].

In previous studies, we have shown in which way compositional and structural modifications caused by introduction of the different amounts of oxygen are governed by the search for global stability to give rise to the crystallization of numerous structures with various compositions and symmetries [9, 10]. The key feature of oxyhydrides is that in the condensed state it allows two and more anions (such as  $O^{2-}$  and  $H^-$ ) to share the common crystalline space through their independent accommodation at the electropositive metal center [1, 2, 5, 6, 9]. As compared with the host metal hydride, the ground state of the oxyhydride system demonstrates better compositional and structural stability; its macroscopic mechanical properties appear to be similar to those of crystalline complex oxides. All together, the anions are committed to successful transformation of the local environment into the complex subsystem of strongly localized charges that may facilitate the dynamically changing interplay of the anions of different structural

units [9, 11]. This opens a large potential in the development of the functional properties associated with optical and electronic responses. In particular, one can refer to experimental reports on the discovery of persistent photoconductance and light-induced reversible colour change [12] as well as the effect of lattice contraction [13]. The analysis of photochromic properties of the yttrium oxyhydrides has shown that the valence electrons effectively deal with the charge and structural complexity [10]. It was also established that upon direct oxidation of the host metal hydride the feasible range of its materials properties can be largely extended [9]. At the system level, this change is of crucial importance because by mounting new lattice architectures it expands the limits of the host geometry. Focus of the further experimental work was given to studies of the electronic and optical properties. The several characteristics of the electronic structure were evaluated from UV-vis spectrophotometry [14] and optical ellipsometry [15] studies. However, investigations of the photochromic effect indicated that it is still little known how the illumination with UV/visible light stimulates respective optical responses as, for example, the reversible change of the color of an oxyhydride film [16, 17]. Moreover, in a number of studies there appeared difficulties in conceptual interpretation of experimental data in terms of the structure-property relationships. The objective of this work is to describe and connect with experiment the results of computational simulations of optical properties. As oxygen chemistry introduces new functionalities through the complex interplay of various anionic degrees of freedom, we wish to understand how the chemical composition of the condensed oxyhydride system in combination with the specific lattice geometry affect its ability to respond to illumination. Consideration will be given to spectral dependencies of the refractive index, reflectance and transmittance factors which are evaluated in terms of macroscopic electronic dielectric function for two different cases – low- and highly-oxidized yttrium hydrides. The focus of comparative analysis will be on effective phase-integrated structural models whose combined optical behaviour is of significant interest.

\* evgenii.strugovshchikov@ut.ee

† aleksandr.pishtshev@ut.ee

TABLE I. Main crystallographic data [9] of models of the bulk yttrium oxyhydride shown in terms of lattice parameters, unit cell volume  $V$ , density ( $\rho$ ), the shortest interatomic distances, and decomposition reaction enthalpy ( $\Delta H$ ) into two binary compounds  $YH_2$  and  $Y_2O_3$ .

Chem. formula	Cryst. struct.	$a$ (Å)	$V$ (Å <sup>3</sup> )	$\rho$ (g/cm <sup>3</sup> )	Y–H (Å)	Y–O (Å)	$\Delta H$ (kJ/mol)
$Y_4H_{10}O$	$P\bar{4}3m$	5.230	143.03	4.43	2.26	2.29	–250.2
YHO	$F\bar{4}3m$	5.292	148.20	4.75	2.29	2.29	–33.1
	$P\bar{4}3m$	5.385	156.16	4.50	2.39	2.17	–20.3
	$Pnma$	7.538 3.767 5.328	151.29	4.65	2.31	2.24	–31.9

## II. SIMULATION DETAILS, METHODS AND MODELING

The Vienna ab initio Simulation Package (VASP) [18, 19] and projector augmented-wave (PAW) method [20, 21] were used for simulations of the electronic structure and optical properties within the density functional theory (DFT). The calculations employed PAW pseudo-potentials based on the plane-wave basis sets taken as  $4s^2 4p^6 5s^2 4d^1$ ,  $2s^2 2p^4$  and  $1s^1$  for Y, O and H elements, respectively. Non-local exchange effects have been taken into account in the scheme of the range-separated hybrid Heyd-Scuseria-Ernzerhof (HSE06) functional [22–24]. The fraction of the Fock exchange were modeled as for an ion-covalent semiconducting system in terms of the inverse dielectric constant [25–29]  $\epsilon_\infty^{-1}$ . The ion-clamped static dielectric tensor ( $\epsilon_\infty$ ) was obtained according to the procedure of the density functional perturbation theory as implemented in VASP. The  $\Gamma$ -centered optimized  $8 \times 8 \times 8$   $k$ -points grid and 700 eV cutoff energy have been used for the numerical integration. The post-processing analysis has been performed with the aid of the following programming tools: The Vesta program [30] for characterization and visualization of the lattice structures; the IMD software [31] for modeling the optical properties of multi-layer combinations. Macroscopic optical properties were evaluated on the base of calculations of the frequency-dependent complex dielectric function  $\epsilon(\omega) = \epsilon_1(\omega) + i\epsilon_2(\omega)$ . The Elk Code [32] was used for modeling a frequency profile of the 2nd-order susceptibility.

Comparison of experimental studies [16, 17] with the theoretical results [9, 10] showed that the low-oxidized composition  $Y_4H_{10}O$  ( $P\bar{4}3m$ ) along with three polymorphic phases of the highly-oxidized structure YHO ( $F\bar{4}3m$ ,  $P\bar{4}3m$  and  $Pnma$ ) can be chosen as suitable models that are most closely reproduce the lattice architecture of experimental samples. In Table I, we quoted the main crystallographic data predicted in our previous work [9]. We used these data for the models  $Y_4H_{10}O$  and YHO to simulate their electronic structure and optical properties. Note that upon further increase of the oxygen content (when the ratio O/H becomes greater than 1) there occurs the disbalance between the Y–H and Y–O connections which leads to the full destabilization of yttrium oxy-

TABLE II. Comparison of optical properties for the models of Table I;  $\epsilon_\infty$  - electronic dielectric constant,  $n$  - the refractive index,  $E_g^{opt}$  - the value of optical band gap.

Chem. formula	Cryst. struct.	$\epsilon_\infty$	$n$	$E_g^{opt}$ eV	Transition
$Y_4H_{10}O$	$P\bar{4}3m$	7.87	2.81	2.2	direct ( $R$ )
YHO	$F\bar{4}3m$	4.75	2.18	4.9	indirect ( $X-\Gamma/M$ )
	$P\bar{4}3m$	4.71	2.17	4.1	direct ( $X$ )
	$Pnma$	4.71	2.17	4.3	indirect ( $Z-Y$ )

hydride crystal structure [9].

Table II adds new information to the data of Table I. For the given models of yttrium oxyhydrides it specifies the electronic dielectric constants  $\epsilon_\infty$  (together with the estimate of the refractive index) as well as describes two key parameters of light absorption in the optical spectral range: absorption edge (optical band gap  $E_g$ ) and character of the gap. The data of Table II can be compared with those of ion-covalent wide-gap oxide  $Y_2O_3$  [33]:  $E_g = 5.6$  eV and  $n = 1.93$  at 600 nm.

## III. RESULTS AND DISCUSSION

The effect of partial oxidation, which is associated with stoichiometric changes in the anionic hydrogen/oxygen sublattices, directly affects the structural characteristics of the crystal lattice. In the present work, we wish to illustrate how this causes a corresponding change in the structure-optical-property relationships. A theoretical study of the electronic structure with respect to structural modifications of yttrium oxyhydrides is reflected in Figure 1 where we have presented site projected and total density of states ( $DOS$ ), band structure along with the spectral behavior of absorption coefficient. Evaluation of optical properties is given at Figure 2 in terms of spectral dependency of the dielectric function  $\epsilon$ , the refractive index  $n$ , the reflectance  $R$  and transmittance  $T$  spectra.

The electronic band structure of the bulk  $Y_4H_{10}O$  is characterized by the direct band gap located in the  $R$  point (0.5;0.5;0.5) of the Brillouin zone (BZ). The topmost part of the valence band (VB) represented mainly by the H  $1s$ -orbitals has a diffuse structure. The lowest empty states of Y  $3d$  orbitals form the lowest part of the conduction band (CB). The  $2p$  oxygen states, which are strongly hybridized with  $1s$  oxygen states, are red-shifted in energy by 1 and 3 eV from the top of VB. The spectral behaviour of the absorption coefficient  $\alpha$ , shown in the right part of Figure 1, is in a good agreement with the site-projected  $DOS$ -picture for  $Y_4H_{10}O$  with respect to possible electronic transitions. It is also seen that an absorption edge for photon energies in this material lies near 2.2 eV.

When oxygen is incorporated in the large amount, the strong covalency of Y–H connections is necessarily modified by a significant portion of ionicity from the new Y–O connections. In the context of overall matching of two anionic sub-

systems, structural modifications show us that, in accordance with the lattice symmetry rules, there are several ways of how the charge and electronic patterns could be reinstalled to compensate the effect of the electron-electron repulsion between valence shells of both anions. As it follows from Figure 1, an increase of the oxygen content leads to the significant enlargement of the dielectric gap for all three polymorphic phases of YHO. The most stable cubic phase  $F\bar{4}3m$  possesses the indirect band gap of 4.9 eV which is largest in comparison with the  $P\bar{4}3m$  cubic, 4.1 eV, and the  $Pnma$  orthorhombic, 4.3 eV, geometries. The  $P\bar{4}3m$  cubic modification exhibits the direct band gap located in the  $X$  point (0;0.5;0) of BZ. In the orthorhombic structure, the dielectric gap becomes again indirect. Thus, the specific trend showing the interplay between lattice and electronic degrees of order in the highly-oxidized composition YHO can be clearly seen. An increasing incorporation of oxygen causes the growth of  $sp$ -hybridization between the  $2p$  oxygen and  $1s$  hydrogen states. The effect of hybridization extends the mixture of these states from the top of VB downward to more than  $-4$  eV. The lowest part of CB is characterized by mixing between the  $3p$  oxygen and  $4d$  yttrium empty states in which the contribution of the oxygen states appears to be of minor importance. In the context of validation of theoretical calculations, analysis showed that the simulation of DOS given by Figure 1 is in a good agreement with the measured XPS spectra for thin films of composition close to YHO [17].

The right side of Figure 1 presents the comparison how the different structural modifications of the bulk YHO determine the various features of optical absorption. It is interesting to note the particular feature which is common for all YHO phases: the growth of absorption spectra ( $\alpha(\omega)$ ) is markedly limited. This is a direct consequence of the strong Coulomb repulsion between valence shells of different anions. Near the top of VB this repulsion creates a flat region of low DOS intensity with such a devastating effect on performance of the electron transitions. The growth of absorption becomes significant beginning from the photon energies of 5.5 eV and higher, i.e. when the transitions between the  $2p$  oxygen and  $4d$  yttrium electronic states attempt to be dominant.

Based on Figure 2, one observes how the peculiarities of the interband electronic transitions are translated into the optical properties of oxyhydrides with low- and high-oxygen amount. The main difference is the blueshift of the photon absorption edge into the UV region observed for all the phases of the YHO system. We have already highlighted this effect in Figure 1; the effect is caused by the change of the band gap energy as the oxygen content grows larger (Table II). Accordingly, as can be seen from Figure 2, the other optical characteristics are also subjected to blueshifting. Moreover, comparison shows that in the spectral region relating to visible light the bulk  $Y_4H_{10}O$  exhibits a larger refractive index than that of any phase of YHO. The result that the frequency-dependent profiles of reflectance  $R$  and transmittance  $T$  spectra of both yttrium oxyhydrides differ from each other is interesting from a practical point of view. This is due to the fact of structural versatility of oxyhydrides [9]. That is, there occurs a wide range of possibilities and perspectives to elaborate a common-

design-sharing prototype of layered-composite optical system accommodating various phases and compositions of oxyhydrides. For illustration of one of capabilities of such approach we performed simulations of optical responses of a two-layer system which was represented as a layered-composite model combining  $Y_4H_{10}O$  and YHO thin films. The calculated transmission spectrum is shown in Figure 3. For comparison we also presented experimentally-measured transmission spectra for a yttrium oxyhydride film that was synthesized as a heterogeneous sample [17]. To achieve the maximally accurate compliance of simulation data with experiment, a structured model comprised 11% of  $Y_4H_{10}O$  and 89% of YHO was chosen for the spatial distribution of individual thin-film components.

Thus, we demonstrated that it is possible to analyze the experimental transmission spectra through the detail comparison with the results of simulating the similar spectral dependencies. Such theoretical work can allow us to predict both affordable structures and most likely compositions of the films of multi-anion compounds. That is, based on the simulations, we construct a set of optical prototypes which we are further matching with experiment in order to elaborate a pilot model. This enables us not only to obtain extensive information on various aspects of a design, syntheses and functionalization of oxyhydride films but also to overcome the difficulties associated with processes of the partial oxidation.

The next result ensues from the analysis whether a nonlinear optical effect is strong in the crystalline  $Y_4H_{10}O$ . As the system has no inversion center, two features of the electronic band picture determined its choice for the investigation: (i) the band gap lying in the visible light region, and (ii) electronic polarizability being higher as compared with YHO. In the context of 2nd-order optical nonlinearity, the focus was to analyze whether the details of the band structure may afford the asymmetry of the electron transitions that could induce the considerable level of the second-order polarization response to the electric field of the incident light wave. Shown in Figure 4 is the theoretical prediction for the independent component of the second harmonic generation (SHG) susceptibility tensor  $\chi_{xyz}(2\omega, \omega, \omega)$  calculated for the non-centrosymmetric phase of  $Y_4H_{10}O$ . It is seen that  $Y_4H_{10}O$  exhibits a relatively large SHG coefficient for a comparably wide transparency range 500 - 900 nm. Theoretical estimates for the photon energies corresponding  $\lambda = 281$  nm and 647 nm provided the values of  $\chi_{xyz}(2\omega, \omega, \omega)$  as 27.0 pm/V and 82.7 pm/V, respectively. These values are close to the nonlinear optical susceptibilities specific to perovskite ferroelectrics with strong optical nonlinearities [34].

#### IV. CONCLUSION

Recent results in research of oxyhydrides spotlight a principal issue of how material properties of the oxyhydride systems are interrelated with their structural versatility. The idea of the present paper was to conduct a design-oriented constructive analysis to understand how the partial oxidation, stoichiometry effects, and structure distinctions give rise to a system-

atic control of the optical properties of yttrium oxyhydrides. The main aim was to get useful information that would afford to perform the separation of various levels of oxidation in the syntheses to develop a stoichiometric compound with the given amount of oxygen. This would allow to expand functionality and to enhance the efficiency of the oxyhydride systems regarding their possible applications in novel electro-mechanical and optoelectronic devices. As the basis of our research we used two stable compositions,  $Y_4H_{10}O$  and  $YHO$ , which were chosen as effective models reflecting the situation with low and with high amount of chemically bonded oxygen, respectively. To evaluate the key differences in characteristics of both model compositions and their structures we performed the simulations of structure-properties relationships by means of DFT calculations. From numerical simulations we found that the special role of oxygen is that its incorporation in the stoichiometric amount varies largely the electronic and op-

tical properties. Analysis of changes of the optical descriptors allowed us to propose an open configuration scheme of layered-composite optical system which may strongly modify its spectral behavior by combining proper phase components. Our theoretical estimates of 2nd order nonlinear susceptibility have shown that non-centrosymmetric  $Y_4H_{10}O$  may exhibit large potential of optical nonlinearity.

## ACKNOWLEDGMENTS

E.S. acknowledges the support from the European Regional Development Fund. A.P. was supported by the Estonian Research Council grant PRG 347. SZK has received funding from the Research Council of Norway through project 309827. Computational work has been performed by using the Norwegian NOTUR supercomputing facilities through project nn4608k.

- [1] H. Kageyama, K. Hayashi, K. Maeda, J. Attfield, Z. Hiroi, J. Rondinelli, and K. Poeppelmeier, *Nat. Commun.* **9**, 772 (2018).
- [2] F. Takeiri and H. Kageyama, *Nihon Kessho Gakkaishi* **60**, 240 (2018).
- [3] V. Fokin, Y. Malov, E. Fokina, S. Troitskaya, and S. Shilkin, *Int. J. Hydrogen Energy* **20**, 387 (1995).
- [4] V. Fokin, Y. Malov, E. Fokina, and S. Shilkin, *Int. J. Hydrogen Energy* **21**, 969 (1996).
- [5] M. A. Hayward, E. J. Cussen, J. B. Claridge, M. Bieringer, M. J. Rosseinsky, C. J. Kiely, S. J. Blundell, I. M. Marshall, and F. L. Pratt, *Science* **295**, 1882 (2002).
- [6] V. N. Fokin, E. E. Fokina, and S. P. Shilkin, *Russ. J. Gen. Chem.* **74**, 489 (2004).
- [7] T. Yamamoto and H. Kageyama, *Chem. Lett.* **42**, 946 (2013), <https://doi.org/10.1246/cl.130581>.
- [8] Y. Kobayashi, O. Hernandez, C. Tassel, and H. Kageyama, *Sci. Technol. Adv. Mater.* **18**, 905 (2017), <https://doi.org/10.1080/14686996.2017.1394776>.
- [9] A. Pishtshev, E. Strugovshchikov, and S. Karazhanov, *Cryst. Growth Des.* **19**, 2574 (2019), <https://doi.org/10.1021/acs.cgd.8b01596>.
- [10] A. Pishtshev and S. Z. Karazhanov, *Solid State Commun.* **194**, 39 (2014).
- [11] A. Pishtshev, E. Strugovshchikov, and S. Karazhanov, *Materials* **13**, 994 (2020).
- [12] T. Mongstad, C. Platzer-Björkman, J. P. Maehlen, L. P. Mooij, Y. Pivak, B. Dam, E. S. Marstein, B. C. Hauback, and S. Z. Karazhanov, *Sol. Energy Mater. Sol. Cells* **95**, 3596 (2011).
- [13] J. P. Maehlen, T. T. Mongstad, C. C. You, and S. Karazhanov, *J. Alloys Compd.* **580**, S119 (2013), sI : MH2012.
- [14] D. Moldarev, M. Wolff, E. Baba, M. Moro, C. You, D. Primet-zhofer, and S. Z. Karazhanov, *Materialia*, 100706 (2020).
- [15] J. Montero, F. A. Martinsen, M. Lelis, S. Z. Karazhanov, B. C. Hauback, and E. S. Marstein, *Sol. Energy Mater. Sol. Cells* **177**, 106 (2018), sI:IME-12 Delft.
- [16] J. Montero, F. Martinsen, M. Tecedor, S. Karazhanov, D. Maestre, B. Hauback, and E. Marstein, *Phys Rev B. Solid State* **95**, 201301 (2017).
- [17] E. M. Baba, J. Montero, E. Strugovshchikov, E. O. Zayim, and S. Karazhanov, *Phys. Rev. Materials* **4**, 025201 (2020).
- [18] G. Kresse and J. Hafner, *Phys. Rev. B* **47**, 558 (1993).
- [19] G. Kresse and J. Furthmüller, *Phys. Rev. B* **54**, 11169 (1996).
- [20] P. E. Blöchl, *Phys. Rev. B* **50**, 17953 (1994).
- [21] G. Kresse and D. Joubert, *Phys. Rev. B* **59**, 1758 (1999).
- [22] J. Heyd, G. E. Scuseria, and M. Ernzerhof, *J. Chem. Phys.* **118**, 8207 (2003), <https://doi.org/10.1063/1.1564060>.
- [23] A. V. Krukau, O. A. Vydrov, A. F. Izmaylov, and G. E. Scuseria, *J. Chem. Phys.* **125**, 224106 (2006), <https://doi.org/10.1063/1.2404663>.
- [24] T. M. Henderson, J. Paier, and G. E. Scuseria, *Phys. Status Solidi B* **248**, 767 (2011), <https://onlinelibrary.wiley.com/doi/pdf/10.1002/pssb.201046303>.
- [25] A. Alkauskas, P. Broqvist, F. Devynck, and A. Pasquarello, *Phys. Rev. Lett.* **101**, 106802 (2008).
- [26] J. Vidal, S. Botti, P. Olsson, J.-F. m. c. Guillemoles, and L. Reining, *Phys. Rev. Lett.* **104**, 056401 (2010).
- [27] A. Alkauskas, P. Broqvist, and A. Pasquarello, *Phys. Status Solidi B* **248**, 775 (2011), <https://onlinelibrary.wiley.com/doi/pdf/10.1002/pssb.201046195>.
- [28] M. A. L. Marques, J. Vidal, M. J. T. Oliveira, L. Reining, and S. Botti, *Phys. Rev. B* **83**, 035119 (2011).
- [29] J. He and C. Franchini, *Phys. Rev. B* **86**, 235117 (2012).
- [30] K. Momma and F. Izumi, *J. Appl. Crystallogr.* **44** (2011), 10.1107/S0021889811038970.
- [31] D. L. Windt, *Comput. Phys.* **12**, 360 (1998), <https://aip.scitation.org/doi/pdf/10.1063/1.168689>.
- [32] “The Elk Code,” <http://elk.sourceforge.net/>.
- [33] Y. Nigara, *Jpn. J. Appl. Phys.* **7**, 404 (1968).
- [34] V. Atuchin, B. Kidyarov, and N. Pervukhina, *Comput. Mater. Sci.* **30**, 411 (2004).
- [35] H. Wenzl, *Int. Met. Rev.* **27**, 140 (1982).
- [36] F. E. Lynch, *J. Less-Common Met.* **172-174**, 943 (1991).
- [37] G. Sandrock, “Applications of hydrides,” in *Hydrogen Energy System: Production and Utilization of Hydrogen and Future Aspects*, edited by Y. Yürüm (Springer Netherlands, Dordrecht, 1995) pp. 253–280.
- [38] J. P. Perdew, K. Burke, and M. Ernzerhof, *Phys. Rev. Lett.* **77**, 3865 (1996).

- [39] L. Hedin, Phys. Rev. **139**, A796 (1965).
- [40] F. Fuchs, J. Furthmüller, F. Bechstedt, M. Shishkin, and G. Kresse, Phys. Rev. B **76**, 115109 (2007).
- [41] N. Marom, F. Caruso, X. Ren, O. T. Hofmann, T. Körzdörfer, J. R. Chelikowsky, A. Rubio, M. Scheffler, and P. Rinke, Phys. Rev. B **86**, 245127 (2012).
- [42] C. Friedrich, M. Betzinger, M. Schlipf, S. Blügel, and A. Schindlmayr, J. Phys.: Condens. Matter **24**, 293201 (2012).
- [43] E. Sanville, S. D. Kenny, R. Smith, and G. Henkelman, J. Comput. Chem. **28**, 899 (2007), <https://onlinelibrary.wiley.com/doi/pdf/10.1002/jcc.20575>.
- [44] W. Tang and E. Sanville, J. Phys.: Condens. Matter **21**, 084204 (2009).
- [45] M. Born, Am. J. Phys. **23** (1955), 10.1119/1.1934059.
- [46] N. Zapp, H. Auer, and H. Kohlmann, Inorg. Chem. **58**, 14635 (2019), pMID: 31626539.
- [47] K. Yoshimura, C. Langhammer, and B. Dam, MRS Bull. **38**, 495–503 (2013).
- [48] A. Baldi, D. Borsa, H. Schreuders, J. Rector, T. Atmakidis, M. Bakker, H. Zondag, W. [van Helden], B. Dam, and R. Griessen, Int. J. Hydrogen Energy **33**, 3188 (2008), 2nd World Congress of Young Scientists on Hydrogen Energy Systems.
- [49] C. Wang, S. Yi, and J.-H. Cho, Phys. Rev. B **101**, 104506 (2020).
- [50] J. Zhang, J. M. McMahon, A. R. Oganov, X. Li, X. Dong, H. Dong, and S. Wang, Phys. Rev. B **101**, 134108 (2020).
- [51] P. Mikheenko, E. Baba, and S. Karazhanov, “Electrical and magnetic behavior of GdOH thin films: A search for hydrogen anion superconductivity,” (NAP 2019, 2020) pp. 1–7.
- [52] A. S. Barker and M. Ilegems, Phys. Rev. B **7**, 743 (1973).
- [53] M. E. Levinshtein, S. L. Rumyantsev, and M. S. Shur (2001).
- [54] D. L. Wood, K. Nassau, T. Y. Kometani, and D. L. Nash, Appl. Opt. **29**, 604 (1990).
- [55] M. Gajdoš, K. Hummer, G. Kresse, J. Furthmüller, and F. Bechstedt, Phys. Rev. B **73**, 045112 (2006).
- [56] E. Mazhnik and A. R. Oganov, J. Appl. Phys. **126**, 125109 (2019).
- [57] D. Setoyama, M. Ito, J. Matsunaga, H. Muta, M. Uno, and S. Yamanaka, J. Alloys Compd. **394**, 207 (2005).

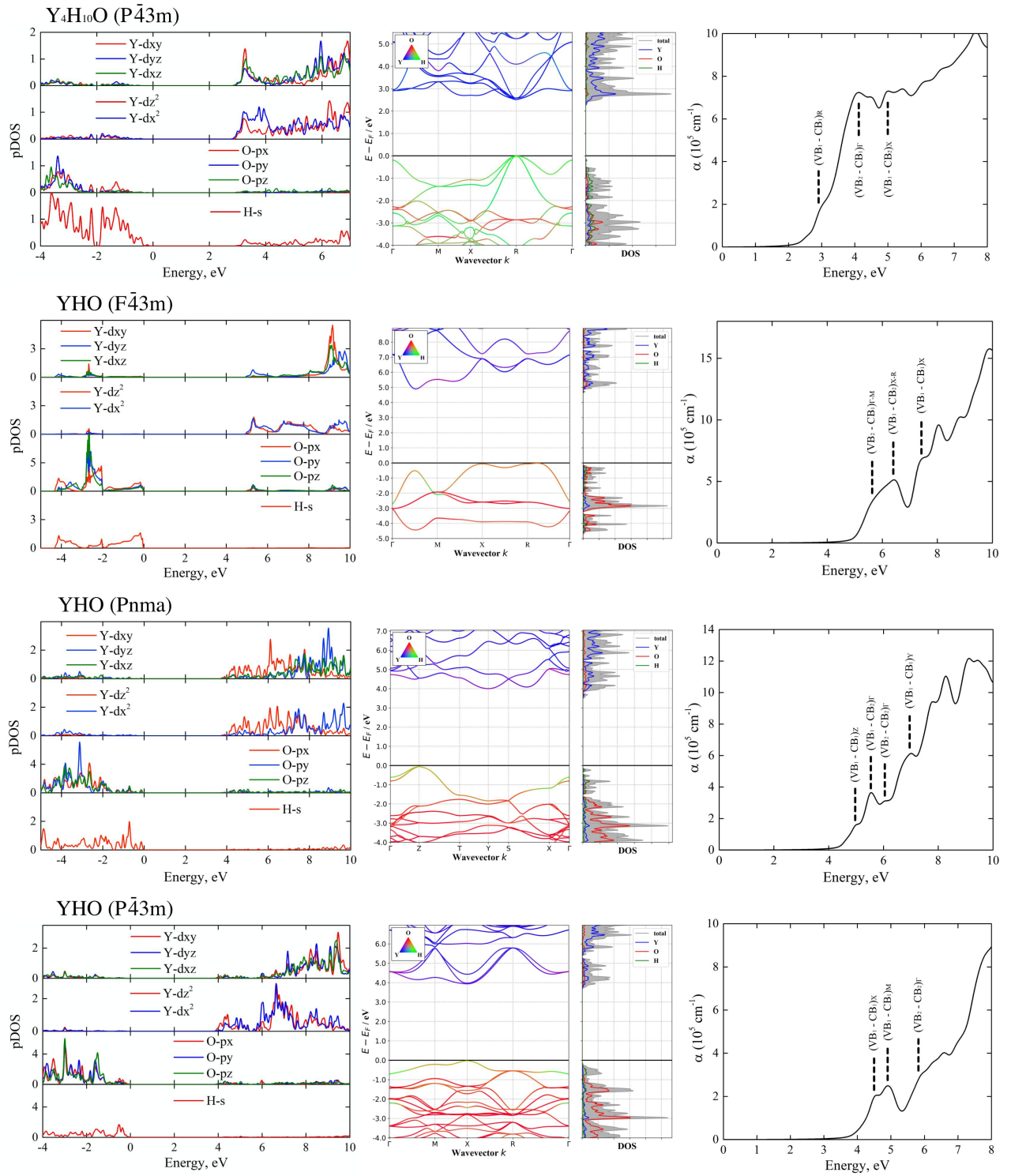


FIG. 1. Site-projected DOS, electronic band structure, and absorption spectra  $\alpha(\omega)$  (the right column) evaluated for the models of  $\text{Y}_4\text{H}_{10}\text{O}$  and YHO systems. The Fermi level is set to the zero-point. The band structure is displayed along the high-symmetry directions of the irreducible BZ.

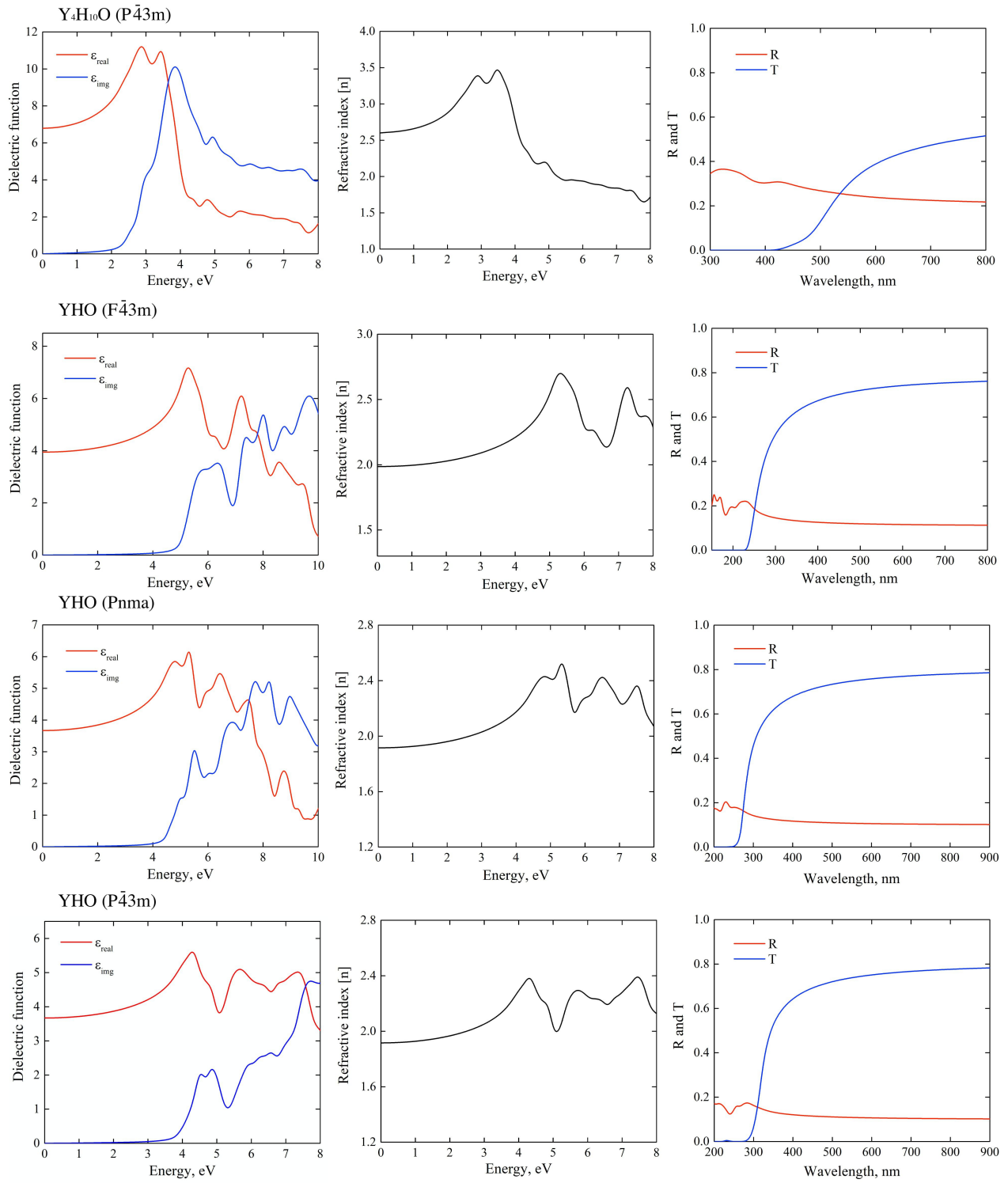


FIG. 2. Spectral behavior of optical characteristics of yttrium oxyhydrides,  $Y_4H_{10}O$  and YHO, simulated in terms of complex dielectric function  $\epsilon$ , refractive index  $n$ , reflectance  $R$  and transmittance  $T$  spectra.

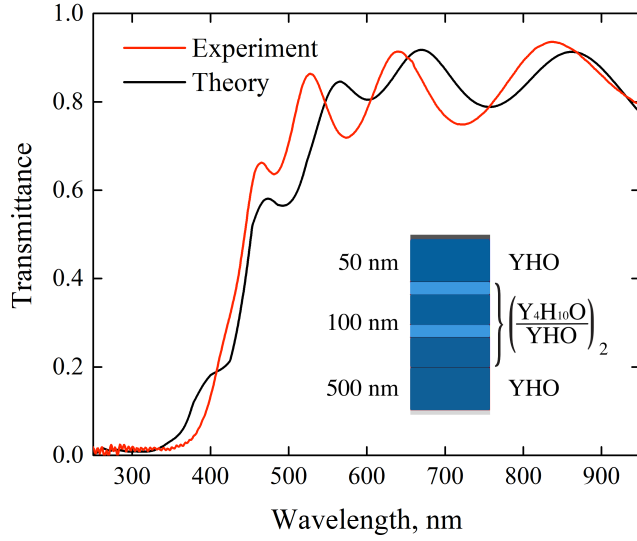


FIG. 3. Simulation of transmittance spectrum of bi-phase composite film (black curve). The model represents a distribution of two compounds: 11% of  $\text{Y}_4\text{H}_{10}\text{O}$  with the  $P\bar{4}3m$  structure and 89% of YHO with the  $F\bar{4}3m$  structure. Red curve corresponds to experimental measurements [17].

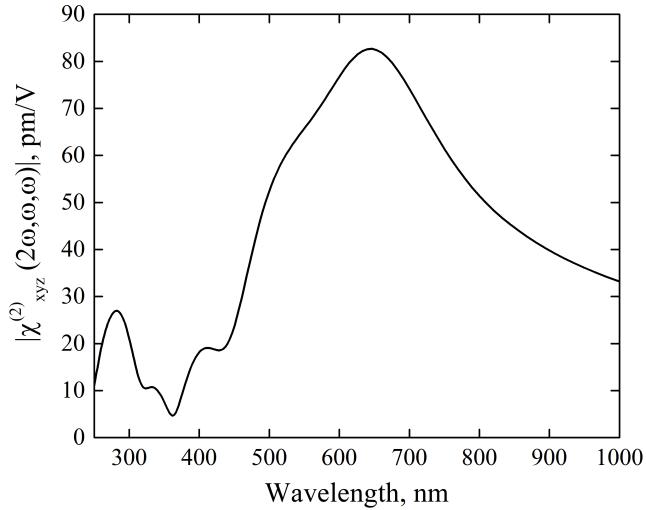


FIG. 4. Theoretical prediction of the SHG spectrum of  $\text{Y}_4\text{H}_{10}\text{O}$  in terms of the spectral behavior of the absolute value of the second-order susceptibility  $\chi_{xyz}(2\omega, \omega, \omega)$ .